# Grid-Connected Integrated Battery Chargers in Vehicle Applications: Review and New Solution

Saeid Haghbin, Sonja Lundmark, Mats Alaküla, and Ola Carlson

***Abstract*—For vehicles using grid power to charge the battery, traction circuit components are not engaged during the charging time, so there is a possibility to use them in the charger circuit to have an onboard integrated charger. The battery charger can be galvanically isolated or nonisolated from the grid. Different examples of isolated or nonisolated integrated chargers are reviewed and explained. Moreover, a novel isolated-high-power three-phase battery charger based on a split-phase permanent-magnet motor and its winding configuration is presented in this paper. The proposed charger is a bidirectional high-power charger with a unity power factor operation capability that has high efficiency.**

***Index Terms*—Grid-connected vehicles, isolated battery charger, review of integrated chargers, split-phase motor.**

## I. Introduction

BATTERIES have a vital role in the development of electrified vehicles. Its energy density, power density, charging time, lifetime, and cost are challenges for commercialization and are still subject of research. The charging time and lifetime of the battery have a strong dependence on the characteristics of the battery charger [1]–[11]. Several manufacturers are working worldwide on the development of various types of battery modules for electric vehicles (EVs) and hybrid vehicles. However, the performance of battery modules depends not only on the design of the modules but also on how the modules are discharged and charged. In this sense, battery chargers play a critical role in the evolution of this technology.

Generally, there are two types of battery chargers: onboard type and stand-alone (off-board) type. However, the onboard charger gives flexibility to charge anywhere where there is an electric power outlet available. The onboard type has the drawback of adding weight, volume, and cost to the vehicle; thus, it is usually made for lower powers ($< 3.5$ kW). When higher charging power is needed, the size and weight of the charger are easier to handle with an off-board charger. Vehicles with a longer EV range (e.g., $> 100$ km) may require filling large amounts of energy (e.g., $> 20$ kWh) in a reasonably short time. Even a 30-min charging time would require a charging power of 40 kW or more, which is on the high side and very well may be limited by the maximum allowed continuous battery power. With a significantly increased fleet of EVs, the need for long charging times, compared to filling e.g., gasoline, implies the need for an unproportionably large amount of charging stations, which will be expensive. Then, high-power onboard chargers are attractive if the weight, volume, and cost can be handled. In that case, the infrastructure requirement would be reduced to rather simple high-power outlets, and thus, the cost of these would be significantly lower than off-board chargers.

There is a possibility of avoiding these problems of additional charger weight, space, and cost by using available traction hardware, mainly the electric motor and the inverter, for the charger circuit, thus having integrated drive system and battery charger. The integration may also allow galvanic isolation. Other aspects to consider regarding integrated chargers are voltage level adaption, unwanted developed torque in the motor during charging, efficiency, low harmonic content in the current from the grid, and mandatory unity power factor operation.

Different types of integrated chargers have been reported [12]–[42], and some of them are reviewed in this paper. Both the hardware and the control algorithm of the reviewed chargers are explained and compared.

In addition, a new isolated-high-power bidirectional battery charger is described, which integrates the traction drive system components (converter and motor) [12], [43]–[48]. A split-phase permanent-magnet motor [49] is used in the proposed integrated charger. The stator has a double set of three-phase windings that are reconfigured once for the traction and charging operations by a relay-based switching device. The motor is rotating during charge operation to eliminate high-magnetization currents compared to other isolated integrated chargers. In the traction mode, the winding configuration makes the machine act like a normal three-phase delta-connected motor. For the charging operation, the windings are reconnected or split so that there are two sets of three-phase windings. One set is connected to the inverter, and the other set is connected to the utility grid after synchronization. While rotating, this split-phase motor acts as an isolated three-phase power source for the inverter to constitute a three-phase boost rectifier (battery charger) with full utilization of the inverter. The system configuration including the motor winding's arrangement in traction and charging modes is presented as well.

Manuscript received February 1, 2011; revised May 24, 2011, August 3, 2011, and December 14, 2011; accepted January 19, 2012. Date of publication February 10, 2012; date of current version September 13, 2012. The work was supported in part by the Swedish Energy Agency and in part by the Swedish Hybrid Vehicle Center.

S. Haghbin, S. Lundmark, and O. Carlson are with the Chalmers University of Technology, 412 96 Gothenburg, Sweden (e-mail: saeid.haghbin@chalmers.se; sonja.lundmark; ola.carlson@chalmers.se).

M. Alaküla is with the Department of Industrial Electrical Engineering, Lund University, 221 00 Lund, Sweden, and also with Volvo Powertrain, 405 08 Gothenburg, Sweden (e-mail: mats.alakula@volvo.com).

Color versions of one or more of the figures in this paper are available online at http://ieeexplore.ieee.org.

Digital Object Identifier 10.1109/TIE.2012.2187414

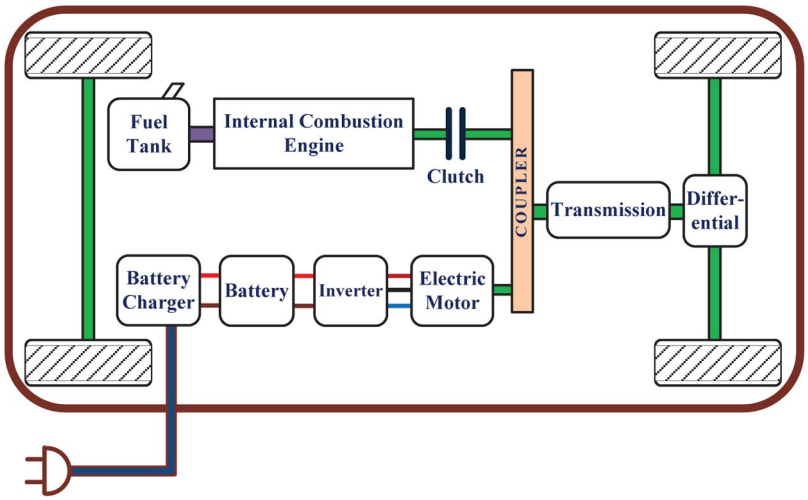


Fig. 1. Simple diagram of a parallel PHEV.

## II. Battery Chargers in Vehicle Applications

Chargers can be classified in terms of power levels and time of charging [50], [51]. The choice of classification depends naturally on nationally available power levels. One example of classification that suits the U.S. residential power source is given in [50]:

1) **Level 1**: common household type of circuit in the U.S. rated to 120 V and up to 15 A.
2) **Level 2**: permanently wired EV supply equipment used specially for EV charging rated up to 240 V, up to 60 A, and up to 14.4 kW.
3) **Level 3**: permanently wired EV supply equipment used specially for EV charging rated greater than 14.4 kW.

Equivalently, the aforementioned categories are known as an emergency charger which charges the battery pack of a vehicle in 6–8 h, a standard charger which charges the battery pack in 2-3 h, and a rapid charger which charges the battery pack in 10-15 min (fast chargers).

Chargers can also be described as either conductive or inductive. For a conductive charger, the power flow takes place through metal-to-metal contact between the connector on the charge port of the vehicle and the charger (off-board charging) or grid (onboard charging). Conductive chargers may have different circuit configurations, but the common issues concern safety and the design of the connection interface.

Inductive coupling is a method of transferring power magnetically rather than by direct electrical contact, and the technology offers advantages of safety, power compatibility, connector robustness, and durability to the users of EVs but on the expense of a lower efficiency and the need of new equipment at charging sites. The EV user may physically insert the coupler into the vehicle inlet where the ac power is transformer coupled, rectified, and fed to the battery, or the charging could be done almost without driver action by wireless charging [52]. For inductive charging, among the most critical parameters are the frequency range, the low magnetizing inductance, the high leakage inductance, and the significant discrete parallel capacitance [53], [54].

Different topologies and schemes are reported for both single- and three-phase input conductive battery chargers [55]–[60]. Usually, the three-phase input solutions are used in high-power applications.

Galvanic isolation is a favorable option in the charger circuits because of safety reasons [61]–[63], but isolated onboard chargers are usually avoided due to its cost impact on the system. As described in [62], if normal nondedicative socket outlets are being used for charging, a residual current device should be used to monitor the earth current for safe operation. Moreover, with a dedicative socket outlet, earth current monitoring is an optional function, as mentioned in the standard. The electrical continuity of the earth conductor should be permanently monitored by the charger, and in the case of loss of electrical continuity of the earth conductor, the charger shall be switched off [63]. In addition, if the traction battery is bonded to the vehicle chassis, the charging system shall provide a galvanic isolation between the mains and the battery [62]. Thus, electrical separation of the traction system and mains supply provides more convenience and freedom to fulfill the standard requirements, beyond increased safety in the system. For example, in nonisolated versions of chargers, a lot of shielding and safety issues should be considered in the whole vehicle electrical system [13], [61] to prevent unwanted earth fault protection trip due to the presence of common-mode currents, noise, and so on. With galvanic isolation, the impact of the high-power converter on the earth path will be drastically reduced.

## III. Integrated Chargers

Fig. 1 shows a schematic diagram of a Plug-in Hybrid EV (PHEV) with parallel configuration (both the internal combustion engine and the electric motor can drive the vehicle simultaneously) as an example of a vehicle with a grid-connected battery charger. The electrical part includes the grid-connected battery charger, battery, inverter, motor, and control system. It is here assumed that, during charging time, the vehicle is not driven and, during driving time, it is not possible to charge the battery pack except for regeneration at braking. In a classical electrical device arrangement in the vehicle, there are separate

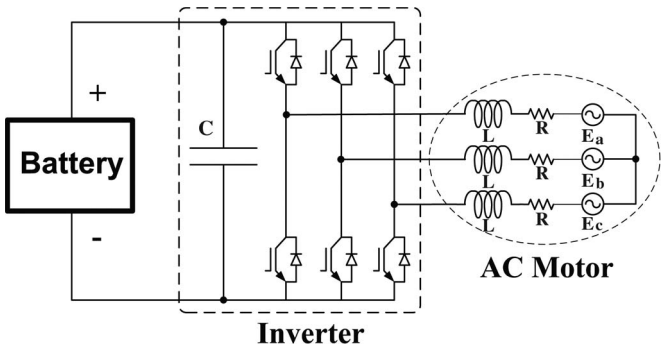


Fig. 2. Electrical traction in a vehicle.

inverter and charger circuits for traction and charging from an external source. However, it is possible to integrate hardware to reduce the number of system components, space, and weight, which is equivalent to cost reduction. For instance, the three-phase three-wire boost ac/dc converter that can be used as a battery charger is very similar to what hardware is available in the traction system. See [55] and [56] for different ac/dc rectifier schemes. Another example of the use of integration is to use the electric motor windings as inductors in the charger circuit. This reduces weight as high current inductors are large components compared to other components like switches.

A traction system based on an ac motor and a three-phase inverter is shown in Fig. 2. In several schemes, a dc/dc converter is used in the system also [64]. The battery power will be transferred to the motor through the inverter. Bidirectional operation of the inverter allows energy restoration to the battery during braking. Regarding different drive systems, different types of integrated chargers are reported both in academia and industry, and some of them are assessed here.

### *A. Combined Motor Drive and Battery Recharge System Based on an Induction Motor*

An integrated motor-drive-and-charger system based on an induction machine was patented in 1994 by AC Propulsion Inc. [13] and is currently in use in the car industry [14]. The main idea is to use the motor as a set of inductors during charging time to constitute a boost converter with the inverter to have unity power factor operation. Fig. 3 shows the functional schematic diagram of this nonisolated integrated charger system. By the means of inexpensive relays, the machine windings are reconfigured to be inductors in the charging mode.

For example, for a single-phase ac supply, LS2 and LS3 shown in Fig. 3 are the induction-motor phase-to-neutral leakage inductances of the windings that act as inductors in the single-phase boost converter circuit. The battery voltage should be more than maximum line–line peak voltage in the input to guarantee unity power factor operation. As an example, they used a 336-$V_{dc}$ battery pack with a 220-$V_{ac}$ input. The relays K1, K2, and K2′ shown in Fig. 3 are used to reconfigure the motor in motoring mode. Furthermore, the inverter switches S1 and S2 are open in the charging mode, and switches S3–S6 are part of the boost converter. A common-/differential-mode filter is used to eliminate the switching ripples and spikes from the line side current. Moreover, a lot of electrostatic shielding is used to decrease the ground current and high-voltage transitions. In the traction mode, relays K2 and K2′ are open and K1 is closed, yielding a classical three-phase drive system.

A conventional three-phase pulsewidth modulation (PWM) scheme is used in the drive-mode operation of the system to generate the desired motor speed and torque. In the battery-charging mode, the PWM scheme with current control is employed to charge the battery with unity power factor capability.

It is possible to have a three-phase input supply with this scheme, but there will be developed torque in the machine during charging that should be considered. The one-phase charger can charge from any source, 100–250 $V_{ac}$, from 200 W up to 20 kW and can be used for vehicle to grid and for backup power and energy transfer to other EVs. The filter bank at the front of the ac supply will smooth the harmonic contents of the charger line current.

Other similar alternatives are patented in the U.S. also [15], [16]. In some examples, the motor, the inverter, and the capacitor components are used in the charging system. All of these solutions are bidirectional nonisolated type of chargers with unity power factor operation and single-phase ac supply. In [15], two solutions are proposed by Rippel in 1990. In the traction mode, an inverter and a three-phase ac motor are used. In the first version, the motor is not used in the charger circuit; instead, an inductor is used to be the energy storage device in the front-end boost converter. The inverter switches are used in the system (part of the boost and dc/dc converter). In a later version, the inductors are eliminated, and the machine leakage inductances are used as part of the charger circuit. When the machine is used as three inductors, the inductors have self-coupling and mutual coupling. Thus, the inductance matrix should be considered in this case. The leakage inductances are the part of the inductors that has no coupling to the other inductances. No switching devices like relays are used to reconfigure the circuit for traction and charging modes (with the same hardware in traction and charging modes).

Another solution patented by Rippel and Cocconi in 1992 (the patent assignee is General Motors Inc.) uses the same idea of integration but there are two independent inverters in the system [16]. They proposed two alternative methods: one with two induction motors and the other one with one induction motor (with double stator windings).

In the first alternative, two induction motors and inverters are used for the traction force. Each motor can be controlled by its dedicated inverter independently. Each motor can be connected to the wheel directly or through a gear that eliminates the need for a transmission and differential in the mechanical system. For the charging mode, the supply will be connected to the neutral point of the motors after electromagnetic interference (EMI) filtering.

The second alternative is using an induction motor with a double set of stator windings comprising two motor halves. The rotor can be coupled to a single wheel or two wheels by means of a reduction-differential gear or a transmission-differential gear. Each winding set is connected to an inverter (each winding

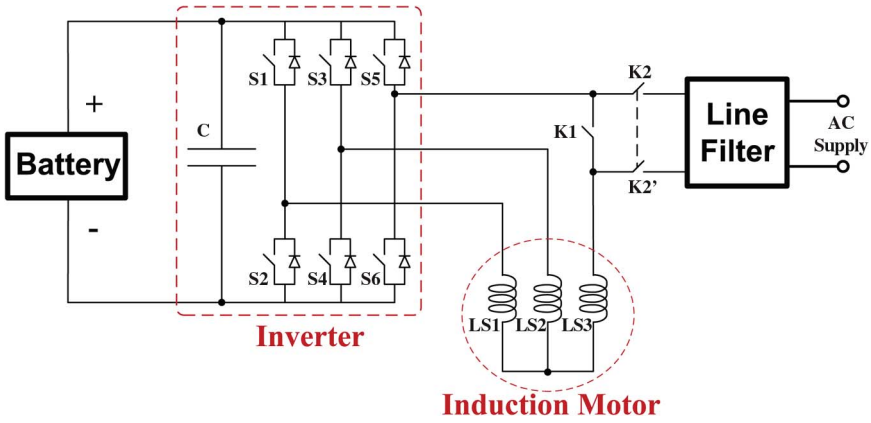


Fig. 3. Nonisolated single-phase integrated charger based on an induction-motor-drive system.

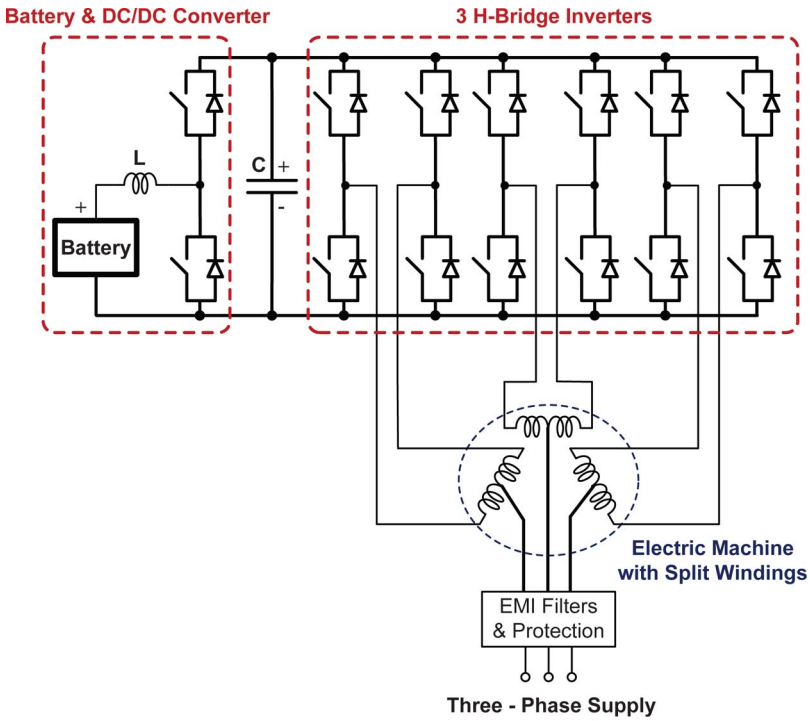


Fig. 4. Three-phase nonisolated integrated charger based on a split-winding ac motor.

set includes three windings). In the charging mode, the supply is similarly connected to the neutral points of the double set of windings after EMI filtering.

For these two alternatives, the detail control scheme is also explained in [16]. A classical PWM control method is used for both the drive and the battery-charging mode. In the drive mode, PWM control of each inverter is such that each phase current is maintained proportional to a sinusoidal reference waveform while the three-phase currents are symmetric with 120° phase shift. The rotor position, currents of two phases, and battery dc voltages are measured and used to generate three-phase reference currents for proper operation of voltage-fed inverters. Each inverter is controlled separately via its own controller. In the battery-charging mode, modulation control is such that, within each inverter, one or more of the phase currents are kept close to the sinusoidal reference, which, in turn, is in phase with the input line voltage for unity power factor operation.

### *B. Nonisolated Integrated Charger Based on a Split-Winding AC Motor*

A nonisolated-high-power three-phase integrated charger is reported by De Sousa *et al.* [17], [18] and Lacroix *et al.* [19] in Valeo Engine and Electrical Systems in 2010. Fig. 4 shows the proposed integrated charger. In the traction mode, a 3H-bridge topology is used with a dc/dc converter. The dc/dc converter consists of an inductor $L$ and two switches. The inverter dc bus voltage is 900 $V_{dc}$ while the battery voltage is maximum 420 $V_{dc}$ for the proposed system. With a traction power of 40 kW, it is possible to charge the battery with 30-kW power in this proposed scheme.

Fig. 5 shows the system equivalent circuit in charging mode. For charging, the three-phase supply is connected to the middle point of the stator windings. A small EMI filter is used to improve the grid current waveforms. As is shown in Fig. 5, there are two 3-phase boost converters sharing a common dc

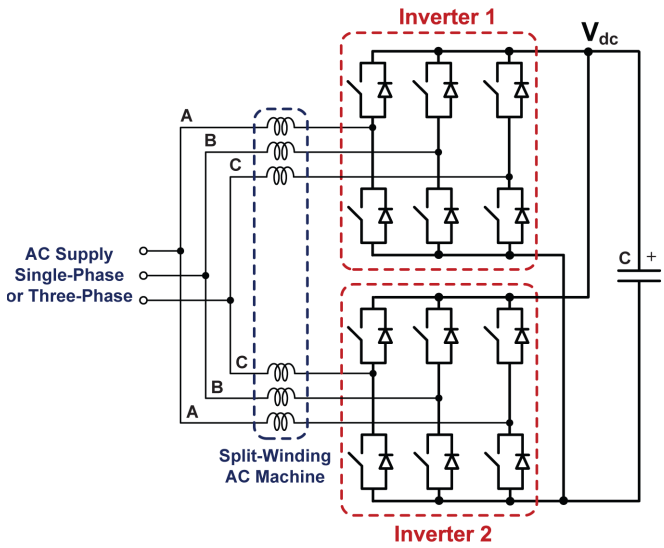


Fig. 5. Charging-mode equivalent circuit of the three-phase integrated charger based on a split-winding ac motor.

bus. By using a split-winding configuration and regulating the same current in the same phases of two boost converters, the developed stator magnetomotive force of the machine is eliminated. Therefore, there is not any rotational magnetic field in the motor during charging.

The proposed charger is a high-power nonisolated version capable of unity power factor operation. There is no need to use a switch like contactor for the charger-to-grid connection. A plug can be used for this purpose. Two international patents are granted for the proposed charger [20], [21].

It is shown that it is possible to use the same strategy for a single-phase supply by Lacroix *et al.* [19]. Fig. 6 shows the system in charging mode for the single-phase supply. Four legs of bridges in the inverter and inductances of two phases are used in this mode. As is shown in this figure, the third H-bridge inverter is not used. The currents will be regulated to be equal for each phase. Unity power factor operation is possible in this case also due to the boost converter topology.

In both the three- and single-phase supplies, there are a front-end power factor correction (PFC) stage and a Buck-type dc/dc converter. An analog PFC is implemented in the first version, and a digital PFC is under development using one-cycle current control scheme [65], [66]. There is no multiplier stage in this control method, and few components are used in the controller. For the Buck converter, a current-controlled PWM method is employed to control the battery charging. The PWM unit switching frequency is 16 kHz in the practical implementation, where the system efficiency is more than 93% at a charging power of 3 kW with a single-phase supply.

### *C. Integral Battery Charger for a Four-Wheel-Drive EV*

An integral battery charger has, in 1994, been reported for a four-wheel-in motor-driven EV by Sul and Lee [22]. The propulsion system includes four induction motors and four three-leg inverters with a battery on the system dc bus. By the use of an extra transfer switch, the whole system will be reconfigured to a single-phase battery charger. Fig. 7 shows the system configuration in traction and charging modes. In the traction mode, four inverters are connected to the system dc bus drive motors (each motor neutral point is float in this mode). In the charging mode (the transfer switch is in position 2), the single-phase ac source is connected between the neutral points of two motors. Utilizing the switches in inverters 1 and 2, this configuration will be a single-phase boost converter with unity power factor operation capability. The third and fourth inverters with the use of two other motors constitute two buck-type converters. Fig. 8 shows the system equivalent circuit in charging mode, where the motors are used as inductors. For each motor, the winding currents are the same for each phase, so there is no developed electromagnetic torque in the motors during the charging time. Furthermore, in the charging mode, by controlling the PWM boost converter, the dc-link voltage is kept constant. The constant-current battery-charging profile is achieved by the control of the two buck-type choppers.

For the front-end boost converter, conventional current-controlled PWM is employed to have rectification with unity power factor. A proportional–integral controller is used to regulate the dc bus voltage. An output feedforward is added to encounter the impact of the input power in current reference determination. The current error is fed to a triangular waveform to generate gate command signals.

A current-controlled PWM scheme is also used for the two parallel step-down buck converters. To reduce the dc bus voltage ripple, the triangular wave is inverted in one converter. Moreover, the buck converters have two modes of operation for battery charging: constant-current and constant-voltage charging modes. In the experimental setup, a PWM frequency of 5 kHz is used for both the boost converter and the buck converter.

### *D. Integrated Charger Based on a PM Motor for an Electric Scooter*

A nonisolated single-phase (110 $V_{ac}$ and 60 Hz) integrated charger for an electrical scooter is another example described in [23]. The author uses the three-phase inverter as a single switch in the charging mode (see Fig. 9). Thus, the switches S2, S4, and S6 shown in Fig. 9 are to be operated all together as a simple switch. In turn, the circuit is a single-phase boost converter. All three windings of the motor are used in the charging process. A power rectifier and a line filter are also used as extra components for the charging operation. It is expected to have unity power factor operation, as is expected for boost converters, and low total harmonic distortion (THD) in the ac line current due to the use of the line filter. A 180-$V_{dc}$ lead–acid battery (12 Ah) is used as the traction power source, and the motor is a 6-kW axial-flux permanent-magnet motor. Moreover, 50-A and 600-V insulated-gate bipolar transistor (IGBT) modules are used with a switching frequency of 25 kHz. At charging mode, the motor is used as three 0.1-mH parallel-connected inductors. The currents through the inductances are thus unidirectional; thus, no torque is developed in the motor, and the rotor can be at standstill.

To charge the battery at the first constant current is applied by the charger, while the battery voltage progressively rises in

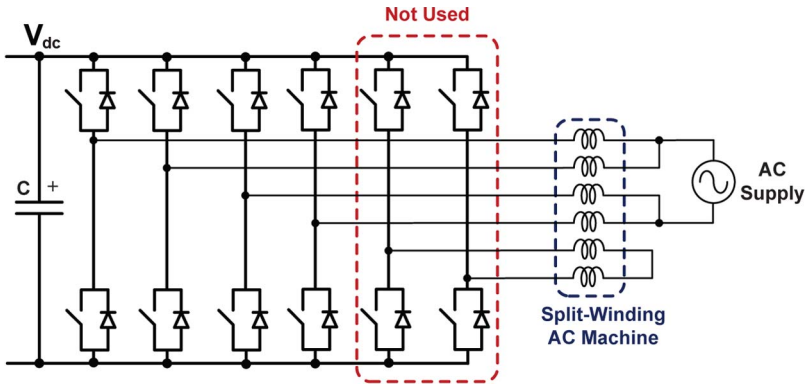


Fig. 6. Charging-mode equivalent circuit of the single-phase integrated charger based on a split-winding ac motor.

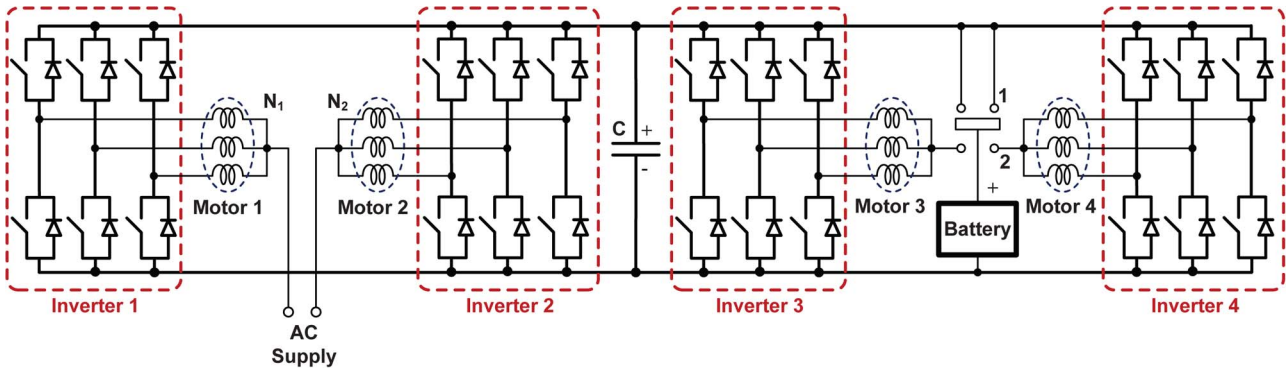


Fig. 7. Single-phase integrated battery charger for a four-wheel-drive system.

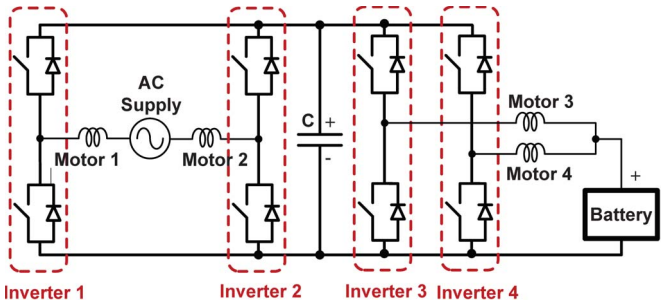


Fig. 8. System equivalent circuit for the four-wheel-drive integrated charger.

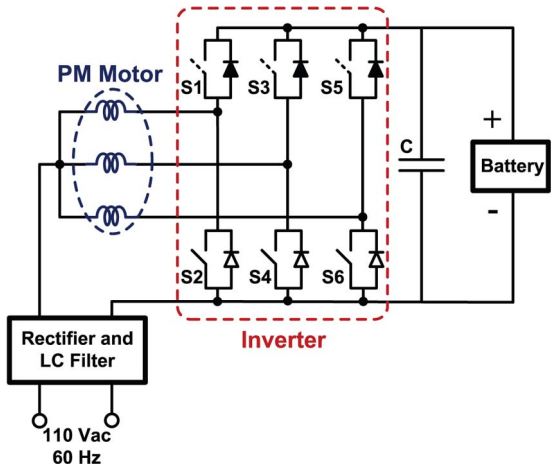


Fig. 9. Single-phase integrated charger based on a PM motor for an electric scooter.

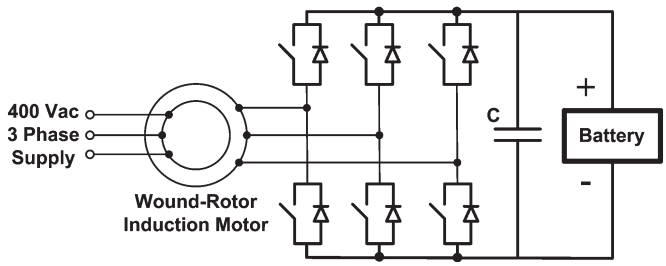


Fig. 10. Three-phase isolated integrated charger based on a wound-rotor induction motor.

this operation. When the battery voltage reaches to a certain level, a constant voltage is applied to the battery as a holding voltage. Discontinuous current mode control is employed for proper charge operation in this system.

### *E. Integrated Charger for a Fork Lift Truck*

An integrated drive/charger system is reported in 2005 for a fork lift truck [24]. In traction mode, a 6-kW induction machine is used to drive the truck. The battery voltage and rated motor voltage are nominal 48 V. A three-phase inverter is utilized for motor control based on the space vector modulation scheme.

In charging mode (see Fig. 10), the motor is used as a low-frequency step-down transformer. A wound-type rotor is used in the drive system, and for the charging mode, the rotor winding is used as a primary side of the transformer that is connected to the three-phase 400-$V_{ac}$ grid. The stator

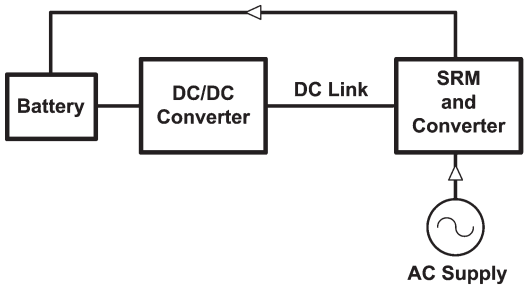


Fig. 11. Single-phase integrated charger based on an SRM drive system.

windings constitute the secondary side of this grid-connected transformer that is connected to the inverter. The inverter serves as a three-phase PWM rectifier for this system in charging mode.

Naturally, there is a galvanic insulation between the grid and the battery by the means of this transformer. The air gap in the motor (transformer in charging mode) will affect the system performance regarding the loss due to the need of large magnetization currents. Other disadvantages are the extra cost of the wound rotor (compared to a squirrel-cage rotor), the need of contactors, and the need to adapt the motor windings to the charge voltage. Advantages include the possibility of bidirectional power flow, low THD, and a unit power factor. The rotor is at standstill during charging, and a mechanical lock is used.

### *F. Single-Phase Integrated Charger Based on an SRM Drive*

Switched reluctance motor (SRM) drive systems are interesting alternatives in vehicle applications due to motor robustness and control simplicity [67]–[70]. An integrated drive-and-charger system for an SRM is reported in [25] for an EV with voltage-boosting and onboard power-factor-corrected-charging capabilities. A boost dc/dc converter is used in the traction mode to boost and regulate the battery voltage for the motor driver. With slight modification of the traction mode, a single-phase nonisolated battery charger is arranged. The dc/dc converter is not used in the charging mode, and by the use of a switch, the system is reconfigured from charging mode to traction mode and vice versa. Fig. 11 shows a simplified diagram of the system in which the power flow in charging mode is through the SRM and its driver to the battery.

The SRM and its driver constitute a single-phase buck–boost converter that ensures unity power factor operation. Two windings of the SRM are used as line filter inductors, and the third one is used as the energy storage inductor in the buck–boost converter. Initially, the battery is charged with a constant current until the voltage rises to a predetermined voltage level. Afterward, a constant voltage is applied to the battery as a holding voltage. The current-controlled PWM scheme is used to keep the charger current in the continuous conduction mode. A PWM switching frequency of 12.5 kHz is used in the practical setup with 500-W charging power.

The proposed integrated charger is a complicated solution in both hardware and control implementation. Moreover, the traction system is not fully utilized in the charger circuit. The dc/dc boost converter and some parts of the SRM and its driver are not used in the charger circuit.

### *G. Single-Phase Integrated Charger Based on a Dual-Converter SRM Drive*

By adding an extra winding that is tightly coupled to the switched reluctance stator windings, it is possible to use it as a step-down transformer. Different versions of single-phase integrated chargers reported by Pollock *et al.* are based on this principle [26]–[28]. Fig. 12 shows a simple basic schematic diagram of the charger. The grid supply is rectified by a diode rectifier module to provide a dc link at the SRM grid-side winding (high-voltage winding). By switching S1, it is possible to have a flyback converter or a forward converter by the use of the SRM driver converter (switches S2 and S3, including their antibody diodes). The SRM grid-side windings have more turns compared to its main winding to adjust battery voltage level and grid voltage.

The unity power factor operation is not feasible in this configuration. The machine core losses are high since the switching frequency is high compared to the 50-Hz nominal frequency. Thus, the system efficiency is not high, and in one example, it was reported to be 25% [28]. The switching frequency of the flyback converter is 1.1 kHz for charge operation. The motor iron lamination is not suitable for high-frequency operation, so it is tried to keep the switching frequency low. The original application was low-power applications like electric shavers, but the topology improved to be used in vehicle application too [28]. The extra winding and switch S1 can drive the machine from the main in the electric shaver application.

### *H. Integrated Bidirectional AC/DC-and-DC/DC Converter for PHEVs*

Conventional hybrid EVs usually have two different voltage levels [71]. A 14-$V_{dc}$ bus is supplied by a 12-$V_{dc}$ battery and a high-voltage 200–600-$V_{dc}$ bus that provides the propulsion power. Traditional loads like lightning systems and vipers are connected to the low-voltage bus. The increasing number of additional loads motivates the car industries to replace the 14-$V_{dc}$ bus with a 42-$V_{dc}$ bus supplied by a 36-V battery. The high- and low-voltage buses are connected to each other by means of an isolated bidirectional dc/dc converter. Also, a dc/ac inverter is used to supply and control the ac drive system.

By combining the dc/dc converter and the battery charger (ac/dc converter), an integrated battery charger was proposed by Lee *et al.* [30]. Fig. 13 shows a simple schematic diagram of the system structure. Moreover, the proposed integrated charger can be identified from this figure. The charger/converter is a nonisolated version with reduced number of inductors and current transducers for the single-phase input supply.

The proposed integrated converter has three modes of operation: battery charging from the grid, boost operation to increase the battery voltage for normal traction operation, and braking operation mode to recover braking power in traction mode. The

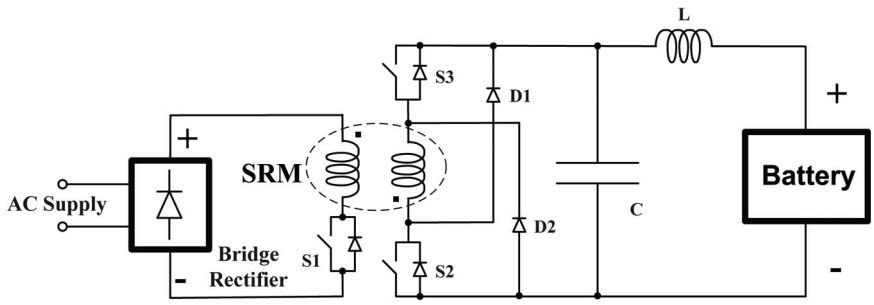


Fig. 12. Single-phase isolated integrated charger based on a dual-converter SRM drive.

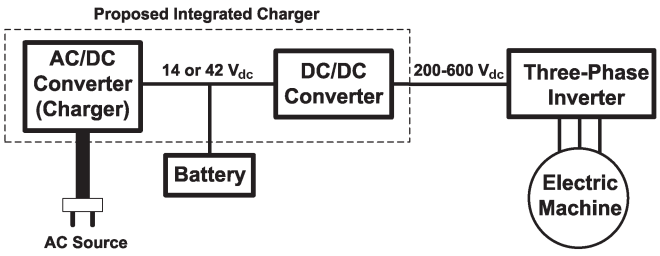


Fig. 13. System diagram of the proposed integrated charger based on the combined bidirectional ac/dc-and-dc/dc converter.

current mode PWM control is used in the system in which detail control operation is explained in [30].

### I. Comparison of Integrated Chargers

Since the reviewed integrated chargers are so different particularly in hardware, it is difficult to find a common ground for a comprehensive comparison. A general comparison of the before-mentioned integrated chargers is presented in Table I with a short summary. Type of supply (three phase or single phase), galvanic isolation of the grid, efficiency, and extra components for integration are considered in this comparison. As shown in the table, there is a column called traction component utilization in charger circuit. For a rough comparison of degree of traction/charger integration, a five-step ranking is used: poor, fair, average, very good, and excellent. Poor means a separate battery charger is used, and excellent means that the traction circuit can exactly be used as the charger circuit without any change or extra components (fully integrated).

## IV. Isolated Integrated Charger Based on the AC Machine Operating as a Motor/Generator Set

As mentioned, isolated-high-power onboard chargers are preferable from a safety viewpoint, but nonisolated ones are still used for cost and weight reasons, like several of those presented earlier. In the following, a drive system with a special machine winding configuration is proposed that can be reconnected into an isolated three-phase integrated charging device in the charging mode through a simple switching device. Fig. 14 shows a schematic diagram of the integrated charger first proposed in [45].

Different motor topologies are possible, concerning both motor type and winding arrangement. One option with an internal permanent-magnet (IPM) synchronous motor (IPMSM) was reported in [45] and [49]. The main idea is to introduce a multiterminal device called motor/generator set to act like a motor in traction mode and like an isolated generator/transformer in charging mode. Fig. 15 shows a simple schematic diagram of the system.

The so-called motor/generator acts as an isolated three-phase power source after synchronization with the utility grid in the charging mode. This rotary three-phase isolated power source constitutes a three-phase boost rectifier (battery charger) with full utilization of the inverter.

This solution has bidirectional capability, so it is possible to feed back power to the grid from the battery. Moreover, unity power factor operation is feasible. The charging power is limited by the motor thermal limit and inverter power limit and limit of the supply, so high-power charging (fast charging) is feasible in this configuration.

### A. System Functional Description

In a two-pole three-phase IPMSM, there are three windings in the stator shifted 120 electrical degrees [72]. For the proposed integrated charger, each phase winding is divided into two equivalent parts; moreover, they are shifted symmetrically around the stator periphery. Basically, there will be six windings inside the stator instead of three for a two-pole machine. Fig. 16 shows the cross section of the motor for the proposed charger in which the winding configuration can be seen in detail. As shown in this figure, there are six windings shifted 30 electrical degrees while the rotor has a two-pole configuration. Other number of pole pairs is also possible.

These six windings can be considered as two sets of three-phase windings. Let us say that $a_1$, $b_1$, and $c_1$ are the first set of windings (the same as classical three-phase windings) and $a_2$, $b_2$ and $c_2$ are the second set of three-phase windings. These two sets of three-phase windings are shifted 30 electrical degrees (the angle between the magnetic axis of $a_1'a_1$, and $a_2'a_2$) in this configuration.

Fig. 17 shows the system in traction and charging modes for a conceptual two-pole machine. In the traction mode, each of the two windings is connected in series in order to constitute a three-phase winding set. These three windings can be connected in $\Delta$ or Y to form a classical three-phase machine. Moreover, the motor is powered by the battery through the inverter. Fig. 17(a) shows the system diagram in this mode. Sensorless schemes, for example, can be employed to run the motor in the traction mode [73]. For the charging mode, the system

TABLE I
COMPARISON OF INTEGRATED CHARGER EXAMPLES

| Solution | Supply | Isolation | Efficiency | Traction component utilization in charger circuit | Extra components for charging | Comments |
|---|---|---|---|---|---|---|
| A combined motor drive and battery recharge system based on an induction motor (III.A) | single-phase or three-phase | non-isolated | high | very good | few relays and a line filter | is currently used in car industry |
| Non-isolated integrated charger based on a split-winding ac motor (III.B) | single-phase or three-phase | non-isolated | high | very good | an extra inverter | will be used in car industry |
| An integral battery charger for a four-wheel drive electric vehicle (III.C) | single-phase | non-isolated | high | very good | a position switch | 4 motors and inverters are used in traction mode |
| An integrated charger based on a PM motor in an electric scooter application(III.D) | single-phase | non-isolated | high | very good | a rectifier and a line filter | the battery voltage should be more than peak line voltage |
| An integrated charger based on a wound-rotor induction motor for a lift truck application (III.E) | single-phase or three-phase | isolated | not high depending on the motor air-gap length | very good | mechanical rotor lock | feasible for wound type rotor induction motor |
| Single-phase integrated charger based on a switched reluctance motor drive (III.F) | single-phase | non-isolated | high | fair | a static switch | both hardware and software are complicated |
| Single-phase integrated charger based on a dual converter switched reluctance motor drive (III.G) | single-phase | isolated | low | average | a bridge rectifier | suitable for low power applications |
| Integrated bidirectional AC/DC and DC/DC converter for PHEVs (III.H) | single-phase | non-isolated | high | fair | some power electronics components | hardware is complicated |

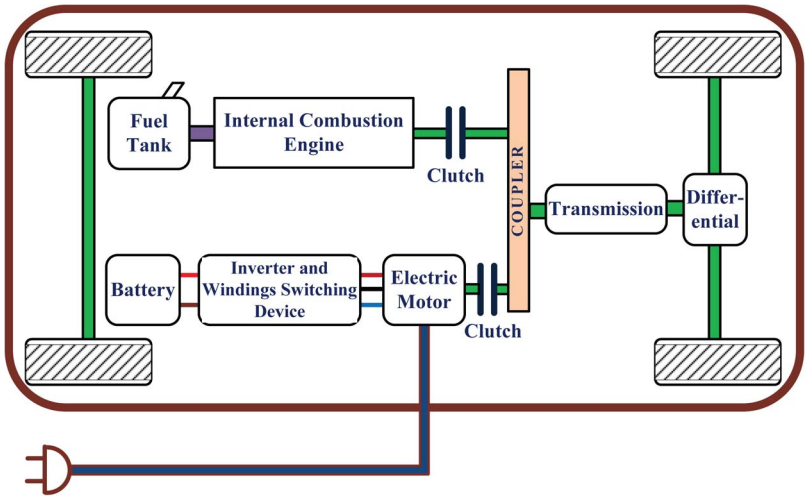


Fig. 14. System diagram of the proposed integrated charger based on the electric machine winding configuration.

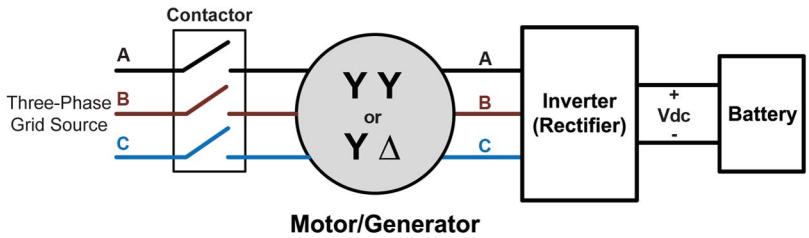


Fig. 15. Isolated-high-power three-phase integrated charger based on a rotating motor/generator device.

is reconfigured according to the scheme shown in Fig. 17(b). A simple relay-based device reconnects the windings, and a contactor is needed to connect the system to the utility grid.

A four-pole IPM machine is designed and optimized for a 25-kW traction system with a possibility to reconnect the windings for charging [44]. Fig. 18(a) shows the winding configuration (in delta) in the traction mode. The dc bus voltage (battery voltage) is 400 $V_{dc}$ in this case. The machine base speed is 1500 r/min while the maximum speed is 6000 r/min. For the charging mode, the windings are rearranged according to Fig. 18(b). Charging power is restricted to half the traction power that is 12.5 kW in this case.

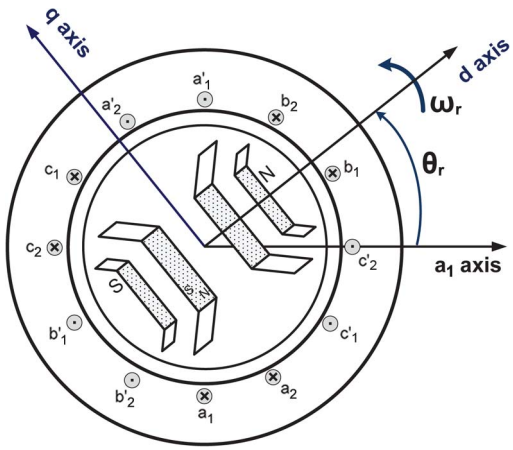


Fig. 16. Cross section of an IPMSM with split stator windings.

If the machine would be kept in standstill during charging, as in [24], the magnetization current will be high due to the air gap. Thus, it is expected to have lower system efficiency, depending on the air-gap length. However, if the machine rotates with the grid synchronous speed, the magnets will induce voltages in the inverter-side windings that emulate an isolated PM ac generator for the inverter. The idea is thus to connect the machine to the grid via the grid-side three-phase windings. These three windings can be used to run the machine as a classical motor. The inverter-side windings will pick up the induced voltage due to the developed flux inside the machine (since they are located on the same pole pair as are the grid-side windings). The inverter can use this isolated voltage source to charge the battery by means of machine inductances as the converter energy storage component (yielding a three-phase boost converter).

To synchronize the machine to the grid, the inverter runs the motor by means of the battery through the inverter-side windings. The grid-side windings are open circuited (the contactor is open), but the induced voltage is measured to be synchronized with the grid voltage.

Grid-side winding voltages and grid voltages are measured and transformed to the $dq$ reference frame. Both voltage vector magnitude and angle of the grid voltage and motor/generator grid-side windings should be equal as an index of synchronization. The voltage magnitude is a function of the motor speed and flux, so by controlling the flux, the voltage level can be adjusted. By controlling the machine speed, the voltage angle is controlled in the grid-side windings.

The motor/generator will rotate at the synchronous speed to meet the frequency synchronization requirement. A clutch is needed to disconnect the motor from the mechanical transmission in charging operation. Moreover, to match the voltage angles, the motor/generator speed reference is controlled to reduce the voltage angle error to an acceptable level.

When the grid-side winding voltages are synchronized with the grid, the contactor is closed, and the grid voltage is thus applied to the grid-side windings. Afterward, the inverter controls the inverter-side winding voltages to charge the battery, which is called charge control here. Now, the inverter-side windings are an isolated three-phase voltage source, and the inverter can control the dc voltage and current at the battery side. By controlling the $d$ and $q$ components of the inverter-side winding's currents, the transfer of both active and reactive powers from/to the grid is controlled during charge operation (after closing the contactor) [44], [47]. It is possible to transfer both active and reactive powers from/to the grid, so unity power factor operation can be achieved.

To have proper boost converter operation, the dc bus voltage should be more than the peak ac line voltage. This can be solved in two ways: using an extra dc/dc converter or $Y-\Delta$ connection of the stator windings to reduce the voltage at the inverter side. The second approach has been selected to reduce the system hardware in this case. The detailed motor design is presented in [49].

The motor rotation is a key point to solve the high-magnetization problem (equivalently, low efficiency) compared to the other solutions (discussed in Section III) where the machine is used as an air-gapped transformer. It is also an advantage that the developed torque can be controlled by the control of the converter. However, this solution needs a switching device for winding reconfiguration, and due to machine rotation in the charging mode, a clutch is needed to disconnect the motor from the mechanical system. System full description including controllers and results are explained in [47].

### *B. Practical Implementation of the Proposed Integrated Charger*

To verify the idea of the proposed isolated integrated charger, a practical setup is designed and implemented based on a 1-kW split-phase permanent-magnet synchronous motor (PMSM). Fig. 19 shows a basic diagram of the experimental system. An available PMSM is re-wound to have two sets of windings, so the motor is not optimized for this application. Nevertheless, it is possible to verify the system functionality with this setup.

First, the contactor is open, and the dc source powers the motor through the inverter. The motor grid-side windings are open, and they pick up the induced voltage due to the rotational electromagnetic force in the stator. A classical sinusoidal-PWM-based field-oriented control (FOC) is used to control the motor with the inverter-side windings. By proper controlling of the motor flux and speed, it is possible to synchronize the motor with the grid in phase and amplitude. When synchronization is finished, the contactor is closed, and grid voltage is applied to the motor. Afterward, it is possible to feed power from the grid to the battery. The inverter currents and dc bus voltage are measured to have FOC of the drive system. The rotor angle is also measured by a resolver and a resolver-to-digital converter (RDC) for the proper voltage vector calculation.

A dSPACE DS1103 controller is used in the setup which is a real-time fast prototype developing control system. The controller is linked to a PC via an Industry Standard Architecture extension bus. The controller digital signals are transistor–transistor logic (TTL) compatible, and the analog input signals are $\pm 10$ V. Hence, suitable measurement interfaces or signal drives are used to adapt different devices to those values.

The inverter type used in the practical setup is SEMISTACK-IGBT, a SEMISTACK family product, from Semikron. The

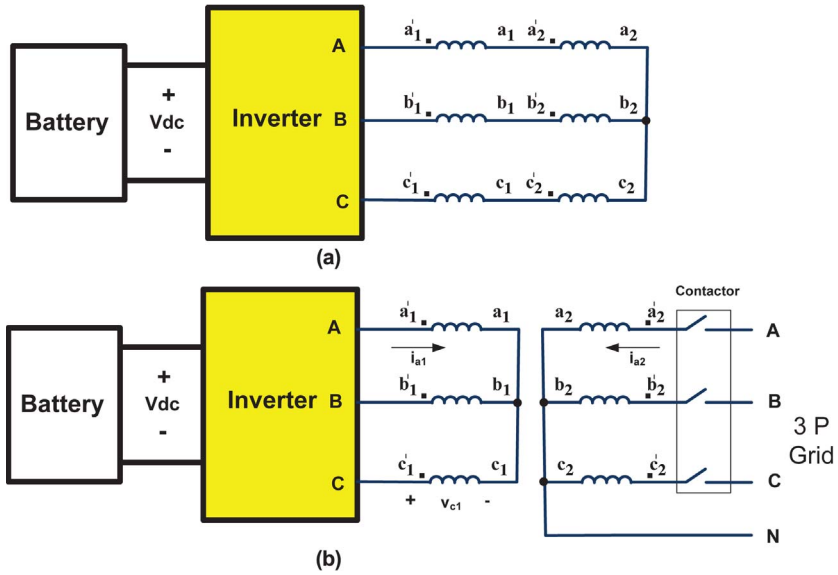


Fig. 17. Proposed integrated charger including an ac motor winding configuration for the conceptual two-pole machine: (a) Traction and (b) charging.

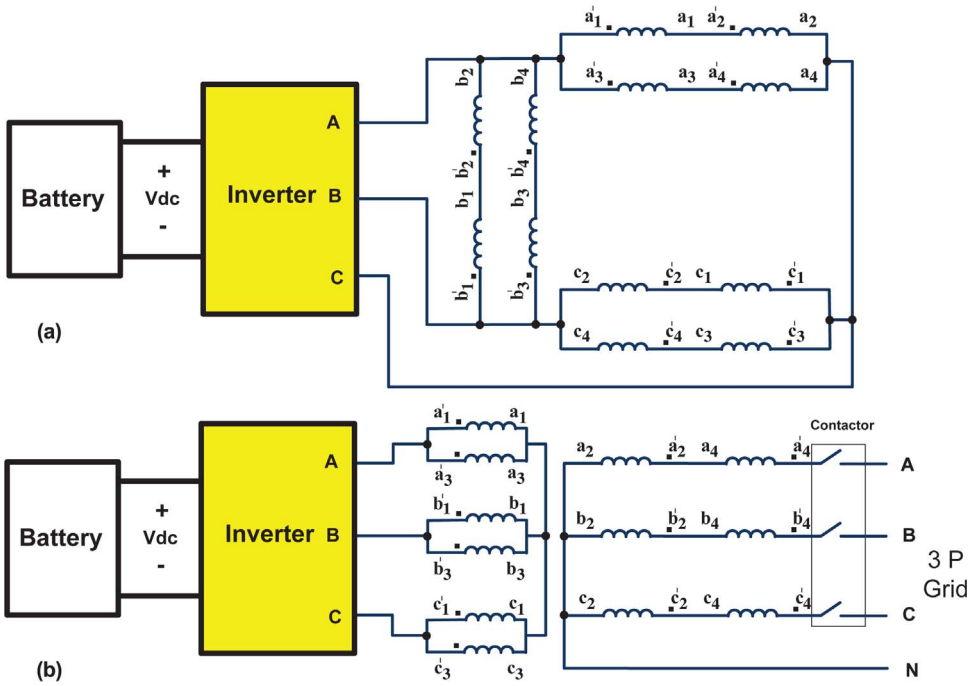


Fig. 18. Practically designed proposed integrated charger with a four-pole and 25-kW rated-power IPM motor: (a) Traction and (b) charging.

inverter rated values are 400 $V_{ac}$/600 $V_{dc}$ and 30 A. The gate signals are isolated from the main power circuit and are triggered by the CMOS level voltages, so a level shifter is used to boost the controller TTL signal to the CMOS level.

The motor is a six-pole machine with a nominal mechanical speed of 1000 r/min. The inertia value is $5.8 \times 10^{-4}$ kg $\cdot$ m$^2$, and the viscous factor is 0.002 N $\cdot$ m $\cdot$ s. The motor inductance value is 30 mH, and the rated current is 1 A for this machine. A resolver transducer is attached to the motor since the machine was originally designed for a servo system.

The dc bus voltage, motor grid-side winding voltages, and grid voltages are measured by designed interface boards. The hardware is based on the AD210 isolated amplifiers. These voltage transducers convert $\pm$400-V signals to $\pm$10-V signals.

Two phases of the inverter currents and the grid currents are measured by current measurement cards. For the current measurement, LEM LA 50-S/SP1 modules are used. This device, with galvanic isolation between the primary and the secondary circuit, outputs a secondary current proportional to the measuring current. A resistor is used to convert this current to a voltage signal suitable for the dSPACE system. The main current in the $\pm$10-A range is converted to a $\pm$10-V voltage signal in these boards.

A printed circuit board (PCB) is designed and fabricated to measure the rotor angle by the resolver. A 6.6-kHz sinusoidal

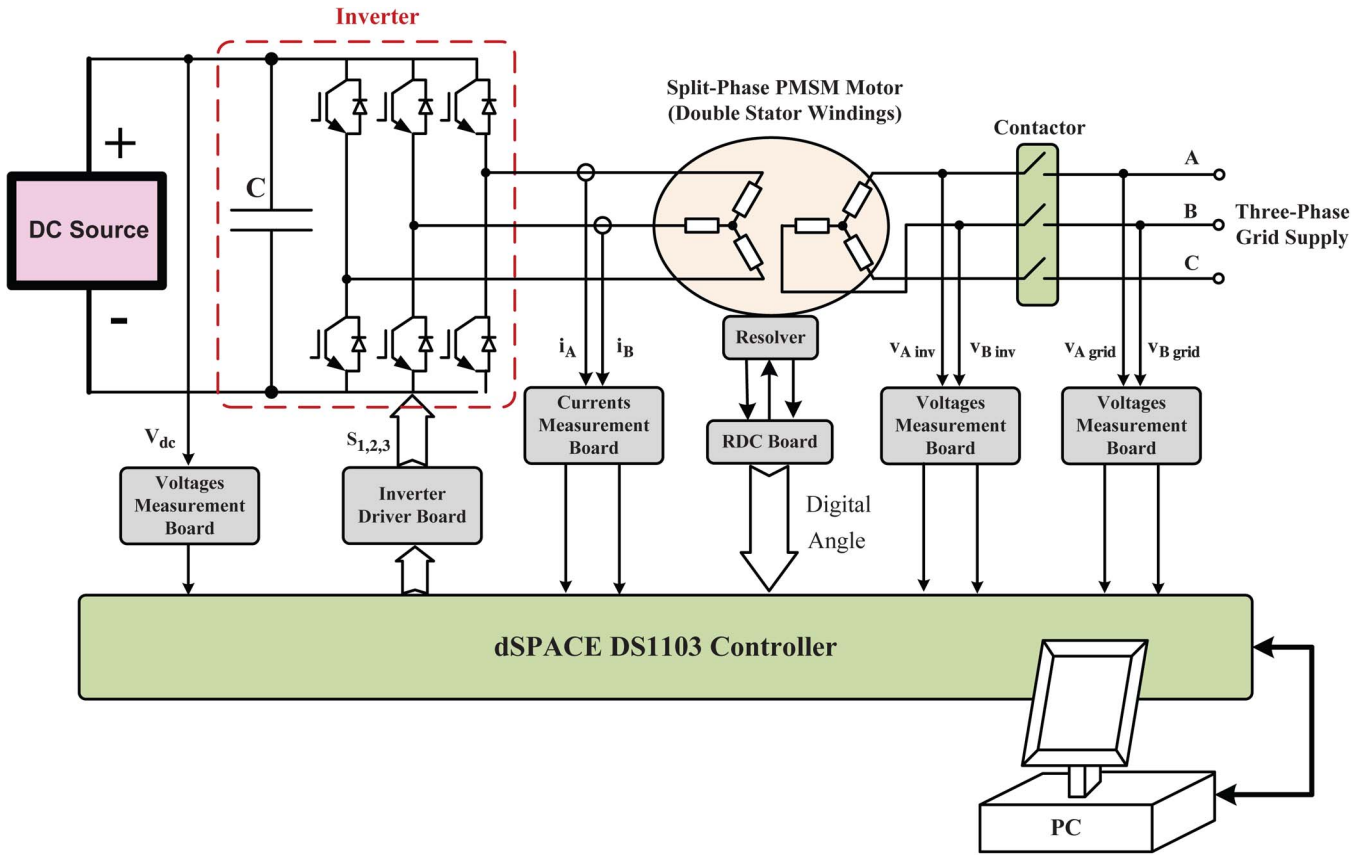


Fig. 19. Block diagram of the experimental system: Integrated motor drive and battery charger.

reference waveform is generated and fed to the resolver rotor coil. The induced voltages on the stator coils are measured and fed to the RDC converter, i.e., AD2S83 in this case, by some interface circuits. The angle is converted to a programmable resolution digital word (12 bit in this case) within RDC operation. The resolution is programmable by the device. The angle in digital form is available at the output port after suitable handshaking operation by the dSPACE system.

Some other hardware components are used in the system that are not explained here such as inverter current protection card, grid connection relay, auxiliary supplies, and so on. Fig. 20 shows a physical layout of the experimental system, and Fig. 21 shows the RDC board.

Using the dSPACE real-time interface, it is possible to fully develop the programs from the Simulink block diagram environment. Thus, the whole software is developed in the Simulink environment. The PWM frequency of the FOC is 12 kHz that is synchronized to the voltage and current measurement instants. This synchronization is vital in order to have a robust control system particularly for the current control loops.

The position is read by the dSPACE system as a digital word. This measured angle is converted to electrical angle by pole-pair multiplication compensation. Moreover, the measured angle is calibrated by offset compensation. In this case, there are two sets of stator windings, so it is possible to measure the grid-side winding voltages for this calibration process.

As mentioned earlier, the motor grid-side winding voltages and the grid voltages are synchronized by adjusting the motor

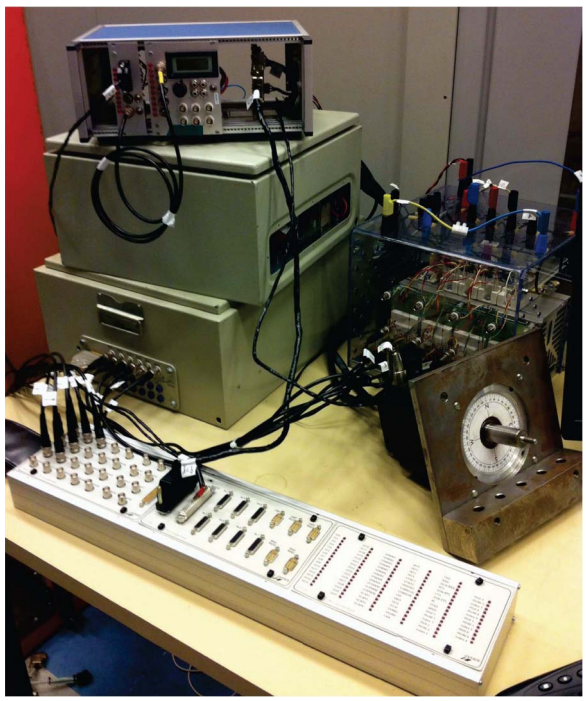

Fig. 20. Experimental system.

speed. Phase A of the voltage for both motor and grid are shown in Fig. 22 before and after the synchronization. At the grid synchronous speed, the motor voltage is not equal to the grid voltage since the motor is not designed for this application.

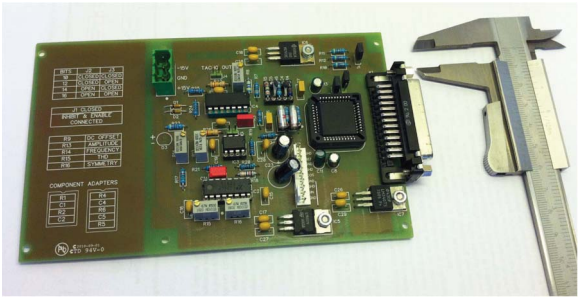

Fig. 21. Resolver-to-digital PCB.

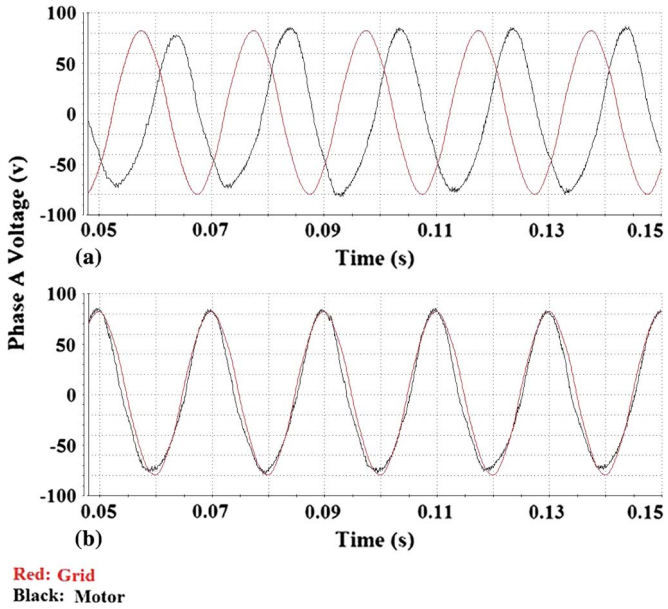


Fig. 22. Motor grid-side winding and grid phase-A voltages. (a) Before synchronization. (b) After synchronization.

Thus, a step-down transformer is used to reduce the grid voltage level close to the motor voltage. The synchronization controller output is a velocity reference signal for the drive system that is converted to the reference values for $d$ and $q$ components of the current by proper control within FOC. When the contactor is closed, the motor is rotating with the grid frequency.

The dc source has been charged with a power level of 300 W at unity power factor operation condition. Moreover, the power transfer from the battery to the grid is also verified.

## V. Conclusion

For vehicles using grid power to charge the battery, charging is happening during the time that the vehicle is parked, so there is a possibility to use the available traction hardware, inverter, and motor in the battery charger system to have an integrated battery-charger-and-drive system. Different integrated chargers reported by industry or academia are reviewed and explained in this paper. Moreover, a novel galvanic isolated-high-power bidirectional integrated charger based on a special electrical machine winding is described. The inverter is fully utilized in the proposed integrated charger, so a minimum number of extra components are needed, including a mechanical clutch used to disconnect the rotating machine from the transmission system during battery charging. Moreover, due to the galvanic isolation from the grid, the charger has higher safety compared to nonisolated versions.

## Acknowledgment

The authors would like to thank K. Khan, M. Leksell, and O. Wallmark of the Royal Institute of Technology (KTH), Stockholm, Sweden, for the design of the internal permanent-magnet motor.

## References

[1] M. M. Morcos, N. G. Dillman, and C. R. Mersman, "Battery chargers for electric vehicles," *IEEE Power Eng. Rev.*, vol. 20, no. 11, pp. 8–11, Nov. 18, 2000.

[2] C. C. Chan and K. T. Chau, "Power electronics challenges in electric vehicles," in *Proc. IEEE IECON*, Nov. 15–19, 1993, vol. 2, pp. 701–706.

[3] A. Emadi, Y. J. Lee, and K. Rajashekara, "Power electronics and motor drives in electric, hybrid electric, and plug-in hybrid electric vehicles," *IEEE Trans. Ind. Electron.*, vol. 55, no. 6, pp. 2237–2245, Jun. 2008.

[4] I. A. Khan, "Battery chargers for electric and hybrid vehicles," in *Proc. Power Electron. Transp.*, Oct. 20–21, 1994, pp. 103–112.

[5] J. G. Hayes, "Battery charging systems for electric vehicles," in *Proc. Inst. Elect. Eng. Colloq. Elect. Veh.—A Technology Roadmap for the Future (Digest No. 1998/262)*, May 5, 1998, pp. 4/1–4/8.

[6] F. L. Mapelli, D. Tarsitano, and M. Mauri, "Plug-in hybrid electric vehicle: Modeling, prototype realization, and inverter losses reduction analysis," *IEEE Trans. Ind. Electron.*, vol. 57, no. 2, pp. 598–607, Feb. 2010.

[7] J. C. Gomez and M. M. Morcos, "Impact of EV battery chargers on the power quality of distribution systems," *IEEE Trans. Power Del.*, vol. 18, no. 3, pp. 975–981, Jul. 2003.

[8] H. van Hoek, M. Boesing, D. van Treek, T. Schoenen, and R. W. De Doncker, "Power electronic architectures for electric vehicles," in *Proc. Elect. Power Train—Emobility*, Nov. 8–9, 2010, pp. 1–6.

[9] S. Vazquez, S. M. Lukic, E. Galvan, L. G. Franquelo, and J. M. Carrasco, "Energy storage systems for transport and grid applications," *IEEE Trans. Ind. Electron.*, vol. 57, no. 12, pp. 3881–3895, Dec. 2010.

[10] Z. Amjadi and S. S. Williamson, "Power-electronics-based solutions for plug-in hybrid electric vehicle energy storage and management systems," *IEEE Trans. Ind. Electron.*, vol. 57, no. 2, pp. 608–616, Feb. 2010.

[11] J. Dixon, I. Nakashima, E. F. Arcos, and M. Ortuzar, "Electric vehicle using a combination of ultracapacitors and ZEBRA battery," *IEEE Trans. Ind. Electron.*, vol. 57, no. 3, pp. 943–949, Mar. 2010.

[12] S. Haghbin and M. Alakula, "Electrical apparatus comprising drive system and electrical machine with reconnectable stator winding," Int. Patent WO/2011/159241, Dec. 22, 2011.

[13] A. G. Cocconi, "Combined motor drive and battery recharge system," U.S. Patent 5 341 075, Aug. 23, 1994.

[14] *AC Propulsion EV Drive System Specifications*, 2008. AC Propulsion Inc. technical note.

[15] W. E. Rippel, "Integrated traction inverter and battery charger apparatus," U.S. Patent 4 920 475, Apr. 24, 1990.

[16] W. E. Rippel and A. G. Cocconi, "Integrated motor drive and recharge system," U.S. Patent 5 099 186, Mar. 24, 1992.

[17] L. De Sousa, B. Silvestre, and B. Bouchez, "A combined multiphase electric drive and fast battery charger for electric vehicles," in *Proc. IEEE VPPC*, Lille, France, 2010, pp. 1–6.

[18] A. Bruyère, L. De Sousa, B. Bouchez, P. Sandulescu, X. Kestelyn, and E. Semail, "A multiphase traction/fast-battery-charger drive for electric or plug-in hybrid vehicles," in *Proc. IEEE VPPC*, Lille, France, 2010, pp. 1–7.

[19] S. Lacroix, E. Laboure, and M. Hilairet, "An integrated fast battery charger for electric vehicle," in *Proc. IEEE VPPC*, Lille, France, 2010, pp. 1–6.

[20] L. De-Sousa and B. Bouchez, "Combined electric device for powering and charging," Int. Patent WO 2010/057892 A1, May 27, 2010.

[21] L. De-Sousa and B. Bouchez, "Method and electric combined device for powering and charging with compensation means," Int. Patent WO 2010/057893 A1, May 27, 2010.

[22] S.-K. Sul and S.-J. Lee, "An integral battery charger for four-wheel drive electric vehicle," *IEEE Trans. Ind. Appl.*, vol. 31, no. 5, pp. 1096–1099, Sep./Oct. 1995.

[23] L. Solero, "Nonconventional on-board charger for electric vehicle propulsion batteries," *IEEE Trans. Veh. Technol.*, vol. 50, no. 1, pp. 144–149, Jan. 2001.
[24] F. Lacressonniere and B. Cassoret, "Converter used as a battery charger and a motor speed controller in an industrial truck," in *Proc. Eur. Conf. Power Electron. Appl.*, 2005, pp. 7–P.7.
[25] H.-C. Chang and C.-M. Liaw, "Development of a compact switched-reluctance motor drive for EV propulsion with voltage-boosting and PFC charging capabilities," *IEEE Trans. Veh. Technol.*, vol. 58, no. 7, pp. 3198–3215, Sep. 2009.
[26] M. Barnes and C. Pollock, "New class of dual voltage converters for switched reluctance drives," *Proc. Inst. Elect. Eng.—Elect. Power Appl.*, vol. 145, no. 3, pp. 164–168, May 1998.
[27] M. Barnes and C. Pollock, "Forward converters for dual voltage switched reluctance motor drives," *IEEE Trans. Power Electron.*, vol. 16, no. 1, pp. 83–91, Jan. 2001.
[28] W. K. Thong and C. Pollock, "Low-cost battery-powered switched reluctance drives with integral battery-charging capability," *IEEE Trans. Ind. Appl.*, vol. 36, no. 6, pp. 1676–1681, Nov./Dec. 2000.
[29] R. M. Davis and W. F. Ray, "Battery chargers in variable reluctance electric motor systems," U.K. Patent GB 1 604 066, 1978.
[30] Y.-J. Lee, A. Khaligh, and A. Emadi, "Advanced integrated bidirectional AC/DC and DC/DC converter for plug-in hybrid electric vehicles," *IEEE Trans. Veh. Technol.*, vol. 58, no. 8, pp. 3970–3980, Oct. 2009.
[31] G. Pellegrino, E. Armando, and P. Guglielmi, "An integral battery charger with power factor correction for electric scooter," *IEEE Trans. Power Electron.*, vol. 25, no. 3, pp. 751–759, Mar. 2010.
[32] G. Pellegrino, E. Armando, and P. Guglielmi, "Integrated battery charger for electric scooter," in *Proc. 13th EPE*, Sep. 8–10, 2009, pp. 1–7.
[33] C. Stancu, S. Hiti, and E. Mundt, "Mobile electric power for medium and heavy duty hybrid electric vehicles," in *Proc. IEEE 35th Annu. PESC*, Jun. 20–25, 2004, vol. 1, pp. 228–234.
[34] F. J. Perez-Pinal and I. Cervantes, "Multi-reconfigurable power system for EV applications," in *Proc. 12th EPE-PEMC*, Aug. 2006, pp. 491–495.
[35] S. Y. Kim, I. Jeong, K. Nam, and H.-S. Song, "Three-port full bridge converter application as a combined charger for PHEVs," in *Proc. IEEE VPPC*, Sep. 7–10, 2009, pp. 461–465.
[36] L. Tang and G.-J. Su, "Control scheme optimization for a low-cost, digitally-controlled charger for plug-in hybrid electric vehicles," in *Proc. IEEE ECCE*, Sep. 12–16, 2010, pp. 3604–3610.
[37] G.-J. Su and L. Tang, "Control of plug-in hybrid electric vehicles for mobile power generation and grid support applications," in *Proc. 25th IEEE APEC*, Feb. 21–25, 2010, pp. 1152–1157.
[38] D. Thimmesch, "An SCR inverter with an integral battery charger for electric vehicles," *IEEE Trans. Ind. Appl.*, vol. IA-21, no. 4, pp. 1023–1029, Jul. 1985.
[39] C. Liaw and H. Chang,, "An integrated driving/charging switched reluctance motor drive using three-phase power module," *IEEE Trans. Ind. Electron.*, vol. 58, no. 5, pp. 1763–1775, May 2011.
[40] A.-T. Avestruz, J. W. Holloway, R. Cox, and S. B. Leeb, "Voltage regulation in induction machines with multiple stator windings by zero sequence harmonic control," in *Proc. 20th IEEE APEC*, Mar. 6–10, 2005, vol. 2, pp. 746–752.
[41] H. Plesko, J. Biela, J. Luomi, and J. W. Kolar, "Novel concepts for integrating the electric drive and auxiliary DC–DC converter for hybrid vehicles," *IEEE Trans. Power Electron.*, vol. 23, no. 6, pp. 3025–3034, Nov. 2008.
[42] L. Shi, A. Meintz, and M. Ferdowsi, "Single-phase bidirectional AC–DC converters for plug-in hybrid electric vehicle applications," in *Proc. IEEE VPPC*, Sep. 3–5, 2008, pp. 1–5.
[43] S. Haghbin, K. Khan, S. Lundmark, M. Alaküla, O. Carlson, M. Leksell, and O. Wallmark, "Integrated chargers for EV's and PHEV's: Examples and new solutions," in *Proc. XIX ICEM*, Sep. 6–8, 2010, pp. 1–6.
[44] S. Haghbin, S. Lundmark, M. Alakula, and O. Carlson, "An isolated high-power integrated charger in electrified vehicle applications," *IEEE Trans. Veh. Technol.*, vol. 60, no. 9, pp. 4115–4126, Nov. 2011.
[45] S. Haghbin, M. Alaküla, K. Khan, S. Lundmark, M. Leksell, O. Wallmark, and O. Carlson, "An integrated charger for plug-in hybrid electric vehicles based on a special interior permanent magnet motor," in *Proc. VPPC*, Lille, France, 2010, pp. 1–6.
[46] S. Haghbin, S. Lundmark, O. Carlson, and M. Alakula, "A combined motor/drive/battery charger based on a split-windings PMSM," in *Proc. IEEE VPPC*, Sep. 6–9, 2011, pp. 1–6.
[47] S. Haghbin, "An isolated integrated charger for electric or plug-in hybrid vehicles," Licentiate thesis, Chalmers Univ. Technol., Gothenburg, Sweden, 2011.
[48] S. Zhao, S. Haghbin, O. Wallmark, M. Leksell, S. Lundmark, and O. Carlson, "Transient modeling of an integrated charger for a plug-in hybrid electric vehicle," in *Proc. 14th EPE*, Aug. 2011, pp. 1–10.
[49] K. Khan, S. Haghbin, M. Leksell, and O. Wallmark, "Design and performance analysis of a permanent-magnet assisted synchronous reluctance machine for an integrated charger application," in *Proc. XIX ICEM*, Sep. 6–8, 2010, pp. 1–6.
[50] M. Rawson and S. Kateley, *Electric Vehicle Charging Equipment Design and Health and Safety Codes*, California Energy Comm., 1998.
[51] K. W. Klontz, A. Esser, P. J. Wolfs, and D. M. Divan, "Converter selection for electric vehicle charger systems with a high-frequency high-power link," in *Conf. Rec. 24th Annu. IEEE PESC*, Jun. 20–24, 1993, pp. 855–861.
[52] C.-S. Wang, O. H. Stielau, and G. A. Covic, "Design considerations for a contactless electric vehicle battery charger," *IEEE Trans. Ind. Electron.*, vol. 52, no. 5, pp. 1308–1314, Oct. 2005.
[53] C. B. Toepfer, "Charge! EVs power up for the long haul," *IEEE Spectr.*, vol. 35, no. 11, pp. 41–47, Nov. 1998.
[54] H. Sakamoto, K. Harada, S. Washimiya, K. Takehara, Y. Matsuo, and F. Nakao, "Large air-gap coupler for inductive charger [for electric vehicles]," *IEEE Trans. Magn.*, vol. 35, no. 5, pp. 3526–3528, Sep. 1999.
[55] B. Singh, B. N. Singh, A. Chandra, K. Al-Haddad, A. Pandey, and D. P. Kothari, "A review of single-phase improved power quality AC–DC converters," *IEEE Trans. Ind. Electron.*, vol. 50, no. 5, pp. 962–981, Oct. 2003.
[56] B. Singh, B. N. Singh, A. Chandra, K. Al-Haddad, A. Pandey, and D. P. Kothari, "A review of three-phase improved power quality AC–DC converters," *IEEE Trans. Ind. Electron.*, vol. 51, no. 3, pp. 641–660, Jun. 2004.
[57] M. Malinowski, "Sensorless control strategies for three-phase PWM rectifiers," Ph.D. dissertation, Warsaw Univ. Technol., Warsaw, Poland, 2001.
[58] E. H. Ismail and R. Erickson, "A new class of low-cost three-phase high-quality rectifiers with zero-voltage switching," *IEEE Trans. Power Electron.*, vol. 12, no. 4, pp. 734–742, Jul. 1997.
[59] V. Vlatkovic, D. Borojevic, X. Zhuang, and F. C. Lee, "Analysis and design of a zero-voltage switched, three-phase PWM rectifier with power factor correction," in *Conf. Rec. 23rd Annu. IEEE PESC*, Jun. 1992, vol. 2, pp. 1352–1360.
[60] H.-J. Chiu, Y.-K. Lo, H.-C. Lee, S.-J. Cheng, Y.-C. Yan, C.-Y. Lin, T.-H. Wang, and S.-C. Mou, "A single-stage soft-switching flyback converter for power-factor-correction applications," *IEEE Trans. Ind. Electron.*, vol. 57, no. 6, pp. 2187–2190, Jun. 2010.
[61] P. T. Krein, "Electrostatic discharge issues in electric vehicles," *IEEE Trans. Ind. Appl.*, vol. 32, no. 6, pp. 1278–1284, Nov./Dec. 1996.
[62] *Electric Vehicle Conductive Charging System—Part1: General Requirements*, 2001. IEC 61851-1, 1st edition.
[63] *Electric Vehicle Conductive Charging System—Part21: Electric Vehicle Requirements for Conductive Connection to an A.C./D.C. Supply*, 2001. IEC 61851-21, 1st edition.
[64] R. Jayabalan, B. Fahimi, A. Koenig, and S. Pekarek, "Applications of power electronics-based systems in vehicular technology: State-of-the-art and future trends," in *Proc. 35th Annu. IEEE PESC*, Jun. 20–25, 2004, vol. 3, pp. 1887–1894.
[65] G. Chen and K. M. Smedley, "Steady-state and dynamic study of one-cycle-controlled three-phase power-factor correction," *IEEE Trans. Ind. Electron.*, vol. 52, no. 2, pp. 355–362, Apr. 2005.
[66] Y. Liu and K. Smedley, "Control of a dual boost power factor corrector for high power applications," in *Proc. 29th Annu. IEEE IECON*, Nov. 2–6, 2003, vol. 3, pp. 2929–2932.
[67] M. Krishnamurthy, C. S. Edrington, A. Emadi, P. Asadi, M. Ehsani, and B. Fahimi, "Making the case for applications of switched reluctance motor technology in automotive products," *IEEE Trans. Power Electron.*, vol. 21, no. 3, pp. 659–675, May 2006.
[68] K. M. Rahman and S. E. Schulz, "High-performance fully digital switched reluctance motor controller for vehicle propulsion," *IEEE Trans. Ind. Appl.*, vol. 38, no. 4, pp. 1062–1071, Jul./Aug. 2002.
[69] H. Hannoun, M. Hilairet, and C. Marchand, "Design of an SRM speed control strategy for a wide range of operating speeds," *IEEE Trans. Ind. Electron.*, vol. 57, no. 9, pp. 2911–2921, Sep. 2010.
[70] J. Liang, D.-H. Lee, G. Xu, and J.-W. Ahn, "Analysis of passive boost power converter for three-phase SR drive," *IEEE Trans. Ind. Electron.*, vol. 57, no. 9, pp. 2961–2971, Sep. 2010.
[71] A. Emadi, S. S. Williamson, and A. Khaligh, "Power electronics intensive solutions for advanced electric, hybrid electric, and fuel cell vehicular power systems," *IEEE Trans. Power Electron.*, vol. 21, no. 3, pp. 567–577, May 2006.

[72] S. E. Lyshevski, *Electromechanical Systems, Electric Machines, and Applied Mechatronics*. Boca Raton, FL: CRC, 1999.
[73] B. K. Bose, *Modern Power Electronics and AC Drives*. Englewood Cliffs, NJ: Prentice–Hall, 2001.

**Saeid Haghbin** received the M.S. degree in electrical engineering from Sharif University of Technology, Tehran, Iran, in 2003 and the Licentiate degree from Chalmers University of Technology, Gothenburg, Sweden, in 2011, where he has been working toward the Ph.D. degree since 2008.

From 2003 to 2007, he worked in industry, mainly on the power electronic systems and automation. His main research interests are motor-drive systems, power electronics, and related signal processing.

**Sonja Lundmark** was born in Gävle, Sweden, in 1966. She received the M.Sc.(Eng.) and Ph.D. degrees from Chalmers University of Technology, Gothenburg, Sweden, in 1992 and 2005, respectively.

Since July 2008, she has been an Assistant Professor with the Division of Electric Power Engineering, Chalmers University of Technology. Her research interests are in the areas of electrical machines and drives and numerical analysis of electromagnetic fields.

**Mats Alaküla** was born in Sweden in 1961. He received the M.S. degree in electrical engineering and the Licentiate degree from Chalmers University of Technology, Gothenburg, Sweden, in 1986 and 1989, respectively, and the Ph.D. degree from Lund University, Lund, Sweden, in 1993.

Since 1994, he has been a Full Professor in industrial electrical engineering with the Faculty of Engineering, Lund University. He is the Coordinator for the Electrical Machines and Drives area in the Swedish Hybrid Vehicles Center. At present, he combines his academic duties with a position as a Senior Specialist in Hybrid Technology at Volvo Powertrain, Gothenburg.

**Ola Carlson** was born in Onsala, Sweden, in 1955. He received the M.Sc. and Ph.D. degrees in electrical engineering from Chalmers University of Technology, Gothenburg, Sweden, in 1980 and 1988, respectively.

He is currently a Professor with the Department of Energy and Environment, Chalmers University of Technology. He has three years of industry experience in the areas of variable-speed systems for wind turbines. His major interests are electrical systems for renewable-energy systems, particularly wind as well as hybrid electric vehicles.